5-2014

Development of a gel based assay to monitor complex formation of tPA with wild type PAI-1 and mutants in the presence of copper

Joanna Nyland
University of Tennessee - Knoxville, jnyland1@utk.edu

Development of a gel based assay to monitor complex formation of tPA with wild type PAI-1 and mutants in the presence of copper

Joanna Nyland

Honor Thesis

Mentor: Dr. Peterson

April 30, 2014

Abstract

PAI-1 (plasminogen activator inhibitor-1) is a serine protease inhibitor (SERPIN) involved in regulation of fibrinolysis, or blood clot dissolution. PAI-1 regulates fibrinolysis by specific inhibition of plasminogen activators, namely tissue type plasminogen activator (tPA). Active PAI-1 uses an exposed loop called the reactive center loop (RCL) to bait proteases like tPA, forming a very stable complex. This influences how much plasminogen is converted into active plasmin and the rate at which blood clots are broken down. In the absence of proteases, PAI-1 converts to a latent, inactive conformation, and this structural change occurs on a half-life of approximately one hour. The Peterson laboratory is interested in the factors that affect how long PAI-1 remains in the active form; too little PAI-1 leads to disease states like fibrosis and embolisms, while too much PAI-1 leads to thrombosis. Interestingly, it has been shown that the addition of metals results in acceleration of PAI-1 to the latent conformation. When a combination of metals and VN are added to PAI-1, the protein remains in the active form significantly longer than just adding VN.

The objective of this study is to determine how metals bind to PAI-1, causing the destabilization of the protein. To address this question we have developed an assay whereby we incubate active PAI-1 with varying concentrations of metals. Upon addition of tPA, only active PAI-1 is available to form a stable complex. By running the mixture on a non-reducing SDS page gel, we can visualize PAI-1/tPA complex formation at the respective metal concentrations. We have previously engineered mutations into PAI-1 in regions suspected to bind metals. We will perform comparisons on PAI-1/tPA complex formation on wild type PAI-1 and on potential metal binding deficient PAI-1 mutants.

Introduction

The physiological function of PAI-1

PAI-1 (plasminogen activator inhibitor-1) is a serine protease inhibitor (SERPIN) involved in regulation of fibrinolysis, or blood clot dissolution (Van De Craen, Declerck et al. 2012). PAI-1 regulates fibrinolysis by specific inhibition of plasminogen activators, namely tissue type plasminogen activator (tPA) (Figure 1) (Olson and Gettins 2011). tPA is a serine protease that cleaves plasminogen to form active plasmin, leading to the breakdown in blood clots (Van De Craen, Declerck et al. 2012). If levels of PAI-1 are too high, thrombosis may incur without regulation (Iwaki, Urano et al. 2012). When levels of PAI-1 are too low, disease states like embolisms and fibrosis may occur (Iwaki, Urano et al. 2012). PAI-1 also controls cellular adhesion, cellular migration and influences the body's inflammatory response to stress (Dellas and Loskutoff 2005). Most of these functions are tied to inhibition of proteases, but others suggest that PAI-1 can function in other ways besides inhibition (Minor and Peterson 2002).

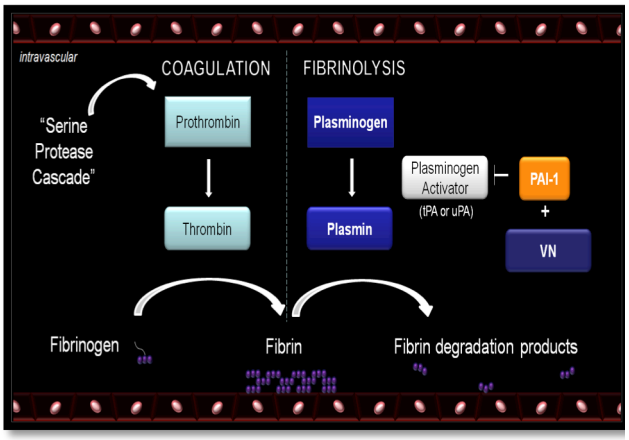

Figure 1. How PAI-1 regulates blood clot dissolution. tPA catalyzes the conversion of inactive plasminogen into active plasmin. Plasmin degrades fibrin blood clots. Conversely, serine proteases also catalyze the coagulation cascade to form blood clots. PAI-1 regulates fibrinolysis by inhibiting serine proteases such as tPA. Vitronectin binds to PAI-1 to stabilize it in the active form and locate it to fibrin clots for function.

PAI-1 utilizes an exposed loop called the reactive center loop (RCL) to inhibit proteases such as tPA (Egelund, Schousboe et al. 1997). The reaction begins with a nucleophilic attack from the active site serine in tPA (Berg 2007). Histidine takes a proton from the serine and

forms an alkoxide ion, making it fit for nucleophilic attack on the scissile bond carbonyl (Berg 2007). A tetrahedral intermediate is formed with a negative charge on the oxygen atom, stabilized by a site called the oxyanion hole from tPA (Berg 2007). The tetrahedral intermediate then collapses, cleaving the arginine-methionine bond in the RCL, forming an acyl-enzyme intermediate (Berg 2007). The remaining RCL then draws across PAI-1, dragging tPA into the central body of PAI-1, completing the inhibition (Olson, Swanson et al. 2001).

PAI-1 exists in an active and latent conformation

Active PAI-1 depends on the RCL being exposed to bait proteases like tPA into forming a stable complex (Egelund, Schousboe et al. 1997). This active state is not the most thermodynamically stable form of PAI-1 (Egelund, Schousboe et al. 1997). Even in the absence of a protease, PAI-1 is prone insert the RCL loop into the interior of the protein body (Stout, Graham et al. 2000). This structural change renders PAI-1 unable to inhibit tPA, and the resulting form of PA-1 is termed the inactive or latent conformation (Stout, Graham et al. 2000). Several regions of PAI-1 are thought to be important in this structural change. The shutter region of PAI-1 (s3A, s5A) must open to allow for the loop to insert into the center of beta sheet A (Buck and Atchley 2005). Unlike what is observed for the inhibition mechanism, the loop must pass through the gate region strands (s3C, s4C, s3B, hG), which open up during latency conversion (Dupont, Blouse et al. 2006). Finally, hF, must be displaced in order for the loop to be fully inserted (Gettins 2002). Additionally, the flexible joints region of PAI-1 is also important because it is the major site of protein-protein interactions (Jensen, Wind et al. 2002).

Factors influencing PAI-1 stability

The stability of PAI-1, or how it remains in the active form, depends on various factors (Figure 2). At physiological conditions, PAI-1 converts to the latent form with a half-life of 1.5 hours (Thompson, Goswami et al. 2010). Lower temperatures generally stabilize PAI-1 in the active form, while higher temperatures increase the rate of latency conversion (Thompson, Goswami et al. 2010). Lowering the pH to around 5.5 has been shown to stabilize PAI-1 in the active form, compared to normal physiological conditions (Sui, Mangs et al. 1999). This has been contributed to the change in protonation state of one or more of the histidines found in PAI-1, specifically His^{354} and His^{143} (Sui, Mangs et al. 1999).

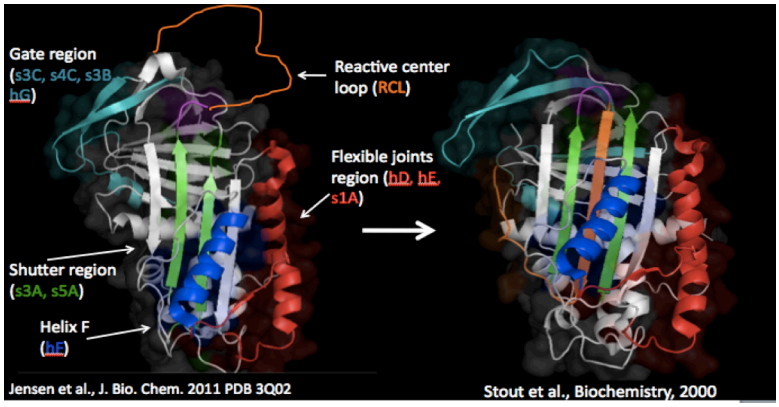

Figure 2. Comparing the differences between active PAI-1 and latent PAI-1. The key regions of PAI-1 important for function are the reactive center loop, shown in orange, the gate region, shown in teal, the shutter region, shown in green, helix F, shown in blue and the flexible joints region, shown in red. The crystal structures of the active form (pdb code: 3Q02) and of the latent form (pdb code:1DVN) highlight the major differences in the key functional regions of PAI-1 due to latency conversion.

Additional stability has been demonstrated by engineering specific mutations within the amino acid code. The 14-1b PAI-1 variant is the most stable, having four mutations: N150H, K154T, Q319L, and M354I, leading to a 30-fold increase in stabilization compared to the wild type PAI-1 (Stout, Graham et al. 2000). An important caveat to studying this mutant is that it not a thermodynamic equivalent to wild type (Jensen, Thompson et al. 2011). A single mutation in the shutter region (W175F) results in a more modest stabilization relative to the wild type form of PAI-1, but W175F PAI-1 possesses a comparable melting temperature to wild

type (Jensen, Thompson et al. 2011). Recently, the crystal structure of this single point mutant was determined in the active conformation (Jensen, Thompson et al. 2011), and this makes it the best model for structural study of wild type PAI-1 to date..

Structural studies on PAI-1 have been difficult due to the rapid conversion of PAI-1 from the active to latent forms. Also, the RCL of PAI-1 is largely disordered, and this part of the structure can not be observed by X-ray diffraction (Jensen, Thompson et al. 2011). First, the latent form of PAI-1 structure was determined, followed by structures of the active form in which multiple mutations were included to stabilize it (Egelund, Schousboe et al. 1997). The crystal structure of active PAI-1 was determined via the mutation W175F, which delayed the latency conversion (Jensen, Thompson et al. 2011). It has a core fold with 3 β-sheets, α-helices and a RCL that is easily accessible to bind to proteases (Jensen, Thompson et al. 2011). PAI-1 has a gate region that opens when converting to latent form in order for the RCL loop to pass through and subseuqently insert (Dupont, Blouse et al. 2006). The N-terminal half of the RCL inserts through the opened shutter region (Egelund, Schousboe et al. 1997). Helix F is moved to allow for the opening of the shutter region and then goes back to its original conformation (Gettins 2002). The flexible joints region is the area where vitronectin and other molecules bind to PAI-1 (Zhou, Huntington et al. 2003).

PAI-1 stability is also influenced by the presence of ligands and binding partners. Vitronectin, a glycoprotein that promotes cell adhesion and spreading, also binds to PAI-1 very tightly (Kd ~ 1nM) (Blouse, Dupont et al. 2009). VN binds to PAI-1 in the flexible joints region, and this results in a modest stabilization of PAI-1 (1.5-2 fold increase) (Thompson, Goswami et al. 2010). PAI-1/VN interaction is required for localization to sites of injury (Stoop, Lupu et al.

2000). Unfortunately, VN has a disordered domain that makes studying its structure difficult (Lynn, Heller et al. 2005). Even so, our lab has determined the crystal structure of the N-terminal somatomedin B domain (Horn, Hurst et al. 2004). This domain is important because it is the major binding interface between VN and PAI-1 (Blouse, Dupont et al. 2009). Towards the C-terminus, there are two domains predicted to have beta propeller structures called the central domain and C-terminal domain (Lynn, Heller et al. 2005). The domains have been modeled together to form a predicted structure using small angle x-ray scattering and neutron scattering techniques, and forms a compact 'peanut-like' three dimensional structure (Lynn, Heller et al. 2005).

The majority of metals are cast into two categories, Type I metals and Type II metals, depending on how they effect PAI-1 (Thompson, Goswami et al. 2010). Type I metals include calcium, magnesium and manganese, and have a small stabilizing effect on PAI-1 (Thompson, Goswami et al. 2010). Type II metals are cobalt, copper and nickel, and have a major destabilizing effect of PAI-1, reducing the half-life to only a few minutes (Figure 3) (Thompson, Goswami et al. 2010). When both Type II metals and VN bind to PAI-1, a major stabilization of PAI-1 occurs (Thompson, Goswami et al. 2010). Through protein fluorescence studies, PAI-1 was shown to

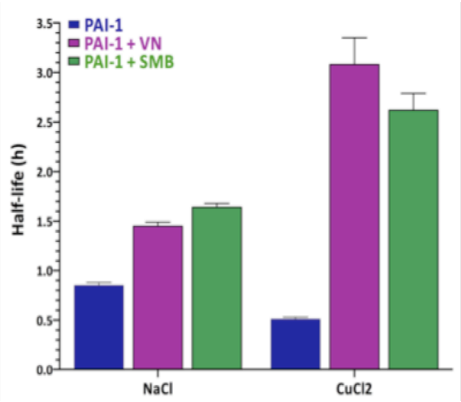

Figure 3. Copper affects on PAI-1 stability with and without vitronectin. PAI-1 in incubated for various time points and then the activity is check by the addition of tPA and tPA substrate. The half life is a measure of how long PAI-1 remains in the active form. The blue bars indicate conditions where PAI-1 is alone. The purple bars indicate where vitronectin is added to PAI-1. Green bars indicate where the SMB domain of vitronectin is added to PAI-1. The two conditions compared were when NaCl was added and when CuCl2 was added.

interact with the two types of metals in different ways, and the metals have a different effect upon the structure of PAI-1 (Thompson, Goswami et al. 2010).

Out of the Type II metals, copper binds to PAI-1 with an approximate 200 times stronger affinity when compared to both cobalt and nickel (Thompson, Goswami et al. 2010). The strong affinity of copper may have large impact in the ability of PAI-1 to regulate plasminogen in the bloodstream. PAI-1 binds copper tightly (~100 nM) and this affinity is well within the range considered as physiologically relevant, with the known concentration of copper in the low micromolar range in the extracellular compartment (Kramer, Kratzin et al. 2001). However, cobalt and nickel are not typically present in the body, so they are not physiologically relevant for study. Interestingly, the disease states arise when there are imbalances in metal concentrations as when there are imbalances in PAI-1 levels (Bleackley and Macgillivray 2011). Some of these diseases are cardiovascular disease, and inflammatory disorders, and platelet leakages making this relevant to study (Bleackley and Macgillivray 2011).

The importance of metal homeostasis in biology

It has been shown that approximately 40% of proteins in the body are only active with metals bound, making metals an essential part of life (Dudev and Lim 2008). Some of the metals commonly found in biological systems are Na^{+}, K^{+}, Mg^{+2}, Ca^{+2}, Zn^{+2}, Mn^{+2}, $Cu^{+1/+2}$, and $Fe^{+2/+3}$. These cofactors perform a variety of functions- specificity, folding, stability, and catalysis. A few examples of the importance of metals in biology are highlighted.

The reaction of DNA polymerase, where DNA molecules are synthesized from nucleic acids, is dependent on two metal ions, usually Mg^{+2} (Berg 2007). One ion binds to the dNTP and

also to the hydroxyl group on the 3' end of the primer. The other ion binds to the 3' hydroxyl group on the primer (Berg 2007). The ion activates the hydroxyl group to attack the α-phosphate on the dNTP and form a bond between the two (Berg 2007). Additionally, the ions stabilize the negative charge from the reaction (Berg 2007). Ca^{2+}, Na^{+}, and K^{+} are a necessary component of muscle contractions (Berg 2007). Na^{+} depolarizes the sarcolemma and causes the action potential in the nerves to continue (Berg 2007). K^{+} is responsible for the repolarization of the cell (Berg 2007). Calcium is released from the sarcoplasmic reticulum of the muscle cell after depolarization and opens up the active site of actin, allowing for the myosin head to attach and the muscles to contract (Szent-Gyorgyi 1975).

Copper is essential for the proper functioning of many enzymes and is regulated by the liver (Kodama, Fujisawa et al. 2012). When the body is unable to regulate the amount of copper in the body, certain disease states arise. Menke's Disease occurs when there is a mutation in the ATP7A gene causing cells in the small intestine and the kidneys to accumulate too much copper leading to a deficiency in copper in the brain (Kodama, Fujisawa et al. 2012). Neurodegeneration occurs from the decrease in cytochrome C oxidase activity from the lack of copper availability (Kodama, Fujisawa et al. 2012). This is because Cytochrome C is an essential member of the electron transport chain that uses the redox potentials of copper and iron to transport electrons, creating an electrochemical gradient and eventually, ATP (Berg 2007). Wilson's disease is caused by a mutation in the ATP7B gene, causing cells to be unable to transport copper into the Golgi apparatus from the cytosol of the cell (Kodama, Fujisawa et al. 2012). Excess free copper is released into the blood stream and accumulates in the liver, leading to liver damage from free radical production (Kodama, Fujisawa et al. 2012). Copper

has also been implicated in the aggregation of α-synuclein, which is associated with Parkinson's disease. Metal catalyzed oxidation of the protein is a result of the interaction between α-synuclein and copper ions (Miotto, Rodriguez et al. 2014).

Where are metals binding on PAI-1?

Copper binds to four to six amino acids at a time: cysteine, methionine, aspartate, glutamate, and histidines (Palm-Espling, Niemiec et al. 2012). Copper II is a divalent cation, meaning that it has two chances of binding to a negative charge (Palm-Espling, Niemiec et al. 2012). Cysteine and methionine contain a neutral sulfur group, which binds to copper (Palm-Espling, Niemiec et al. 2012). Copper has been known to bind to the deprotonated nitrogen on an imidazole group on histidines (Palm-Espling, Niemiec et al. 2012). Copper also binds to negatively charged oxygens in carboxylate groups found on aspartate and glutamate (Palm-Espling, Niemiec et al. 2012). The binding of cysteine to copper is the most common out of all listed above, but there are no cysteines present in PAI-1 (Palm-Espling, Niemiec et al. 2012). Presently, studies are being done to determine which amino acids on PAI-1 copper binds, and how his affects protein structure (Palm-Espling, Niemiec et al. 2012). The

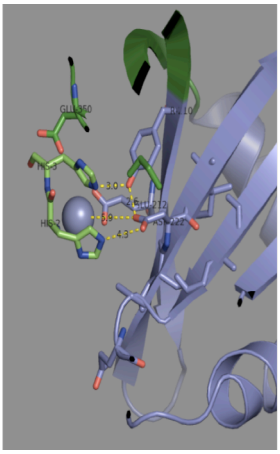

Figure 4. The W175F crystal structure region where zinc binds PAI-1. The green residues are coming from the N-terminus of one PAI-1, residues H2 and H3. The purple residues are coming form the gate region of a second PAI-1, residues D222, E212, E242, and E350. They form an asymmetric dime to bind a zinc ion. The pdb code for this crystal structure is 3Q02.

sequence of PAI-1 contains 15 methionines, 35 residues containing carboxylic acid groups (D, E) and 12 histidines (Van De Craen, Declerck et al. 2012).

The crystal structure of the W175F mentioned previously contains two molecules of PAI-1 bound together via a zinc ion (Figure 4) (Jensen, Thompson et al. 2011). The ion binds to 2 histidines (H2 and H3) from the N-terminal site of one PAI-1 molecule and the also to three gate region carboxylate containing residues (E212, D222, E350) (Jensen, Thompson et al. 2011). These binding sites have lead to questions: Where on PAI-1 does metal binding have a large effect on the stability of the molecule? Does metal binding have an effect on the conformation of the protein? Do metals have an impact on the binding of VN and PAI-1?

The objective of this study is to determine how metals bind to PAI-1, causing the destabilization of the protein. To address this question we have developed an assay in which active PAI-1 is incubated with metals in varying concentrations. Upon addition of tPA, only active PAI-1 is available to form a stable complex. By running the mixture on a non-reducing SDS page gel, we can visualize PAI-1/tPA complex formation at the respective metal concentrations. We have previously engineered mutations into PAI-1 in regions suspected to bind metals. We will perform comparisons on PAI-1/tPA complex formation on wild type PAI-1 and on potential metal binding deficient PAI-1 mutants.

Our goal has been to observe the amount of complex formation for wild type PAI-1 under increasing metal concentrations to determine the critical concentration of metal causing latency conversion. The different amino acid substitutions were introduced, based upon the W175F crystal structure (Jensen, Thompson et al. 2011). We hypothesize that if any of the residues are involved in metal coordination, we will observe less of an effect on complex

formation with tPA compared with wild type PAI-1. In other words, on the gel we should see complex formation at higher free metal concentrations. We used charge reversal single mutations and alanine mutants for double and triple mutants. We suspect these changes will disrupt metal coordination if it is taking place through those residues.

Methods

Mutagenesis

Primers were developed to be complementary to the template strand of the PAI-1 gene with a specific mismatch mutation. Polymerase chain reaction (PCR) was performed by first exposing the reaction to 95°C to denature the double stranded DNA. Then, nucleotides, buffers, primers, polymerase, and magnesium were added to the DNA strands. The temperature was lowered to 45° C for annealing of the DNA strands to occur. The temperature was then raised to 72° C to extend the primers with dNTP's. These three steps were repeated for 35 cycles. A Dpn1 digest was performed to remove the DNA without the mutation by cleaving the methylated DNA, leaving only the DNA with the incorporated mutation.

The DNA was transformed into DH5-α cell line. The cells were heat shocked at 42° C to allow for DNA entry followed by incubation on ice for 2 minutes. Next, SOC media was added to grow the cells for 1 hour. The cells were plated on agar plates containing kanamycin and grown overnight. A single colony was selected and the DNA purified using a mini-prep kit. Finally, we determined that the mutation was incorporated by sequencing the DNA.

Protein expression

The PAI-1 and mutant proteins were produced with a pET 24d expression plasmid DNA. The plasmid was transformed into *Eschericha coli* Rosetta 2 (DE3) pLysS cells (Novagen-EMD) via the heat shock method. The colonies of E. coli grew on agar plates that contained kanamycin and chloramphenicol. A single colony was selected and transferred to liquid culture of terrific broth cell culture media to grow at 37° C with the rotor shaking at 300 rpm. The liquid culture was then subcultured into a larger volume of media. As optical density ($OD_{600)}$ reached 0.8 absorbance units, the temperature was decreased to 15°C. After the OD reached an absorbance unit of 1.0, 1 mM IPTG was added to the culture to induce the expression of the protein by removing the repressor of the lac gene. The cultures were spun down, the supernatant poured off and either were purified immediately or frozen at -80°C for later use.

Purification

PAI-1 and mutant proteins were purified with three different columns. The first used was a sulfopropyl (SP) sepharose column for cation exchange at pH 6.5, using a buffer solution containing 50mM sodium phosphate, 1mM EDTA and 80mM ammonium sulfate. The protein was eluted with an 80-500mM ammonium sulfate gradient to break the electrostatic interactions. The second column was a nickel-charged chelating sepharose for immobilized metal affinity (IMAC), with a buffer solution containing 50mM sodium phosphate, 20mM imidazole and 500mM sodium chloride, and was eluted with a 20-120mM imidazole gradient. Last, a gel filtration column (S-100) sephacryl was used to purify the protein from final impurities on basis of difference in size. After all steps, the fractions were checked at absorbance 280nm and then ran on an SDS-PAGE gel followed by western blotting to confirm the accurate pooling of PAI-1.

P10 buffer exchange column

The column was equilibrated with 15mLs of gel assay buffer containing 100mM ammonium sulfate, 50mM MOPS, and chelated with 5mgs/mL to remove trace metals, with a pH of 7.4 at 37°C to change the protein conditions from the storage buffer to the assay buffer. The proteins were stored in a storage buffer containing 50 mM phosphate buffer, 300 nM NaCl and 1mM EDTA, pH 6.5. In loading phase, 500mL's of PAI-1 in storage buffer was run through the P10 buffer exchange column. In elution phase, 1ml of MOPS gel assay buffer was then run through the column for protein elution. The concentration of the protein was then determined by the absorbance at 280nm, followed use of beers law with an extinction coefficient of 34,280$cm^{-1}M^{-1}$.

Metal Assays

A 3mM copper solution was prepared with MOPS buffer using 1M $CuSO_4$ stock correcting the pH to 7.4 at 37°C. Stock solutions of 200 uM, 500 uM and 2000 uM were made to make several different concentrations of metal to be used in the assay ranging from 200 uM to 3000 uM (making a range of 20 nM to 2037 nM free copper). A stock solution of tPA at 4uM and 12 uM of PAI-1 with MOPS buffer was made. Reactions were made with the same amounts of PAI-1 and tPA, but increasing concentrations of metal to see the effect metals have on complex formation. The reactions were incubated at 37°C for 30 minutes. Then, 10 uL of tPA was then added to each reaction, except for the PAI-1 control. Finally, 7 uL of non-reducing dye was added to each to stop the reaction and boiled for 10 minutes. The assay was run on a non-reducing SDS-PAGE at 150V for 1 hour on a 4-12% Bis-Tris gel with 1x NUPAGE MOPS. The gels

were stained with Commassie Blue followed by destaining, imaging and subsequent densitometry.

Results

The metal assays were performed to determine the effect of increasing concentrations of copper on the conversion of PAI-1 from the active state to the latent state. With the addition of tPA, only active PAI-1 will be available to form the complex. When run on a non-reducing SDS page gel, visualization of the PAI-1/tPA complex formation is easily differentiable over the copper concentration range tested. With the increase of copper concentration, we expect to see more PAI-1 in the latent form over the 30-minute timespan and less of it will be able to bind to tPA. We are trying to determine the copper concentration that causes this effect.

An example gel is shown from an assay using wild type PAI-1 (Figure 5). Lane four on the gel contains the ladder, which sets the protein molecular weight standards, ranging from 11kDa to 170kDa. The first lane is a control with only PAI-1 to show that it migrates near the 43kDa standard. The second lane is a control with only tPA to show that it migrates near the 70kDa standard. The third lane contains both tPA and PAI-1 and contains migration of the PAI-1/tPA complex in-between the 96kDa and 130kDa standard, consistent with a total mass of 113kDa for the migration of the complex. All samples are subjected to thirty minutes incubation at 37°C followed by addition of tPA to form complex.

The subsequent lanes (5-13) have increasing concentrations of free copper: 20nM, 50nM, 100nM, 150nM, 200nM, 501.5nM, 1008nM, 1520nM, and 2037nM. There are three

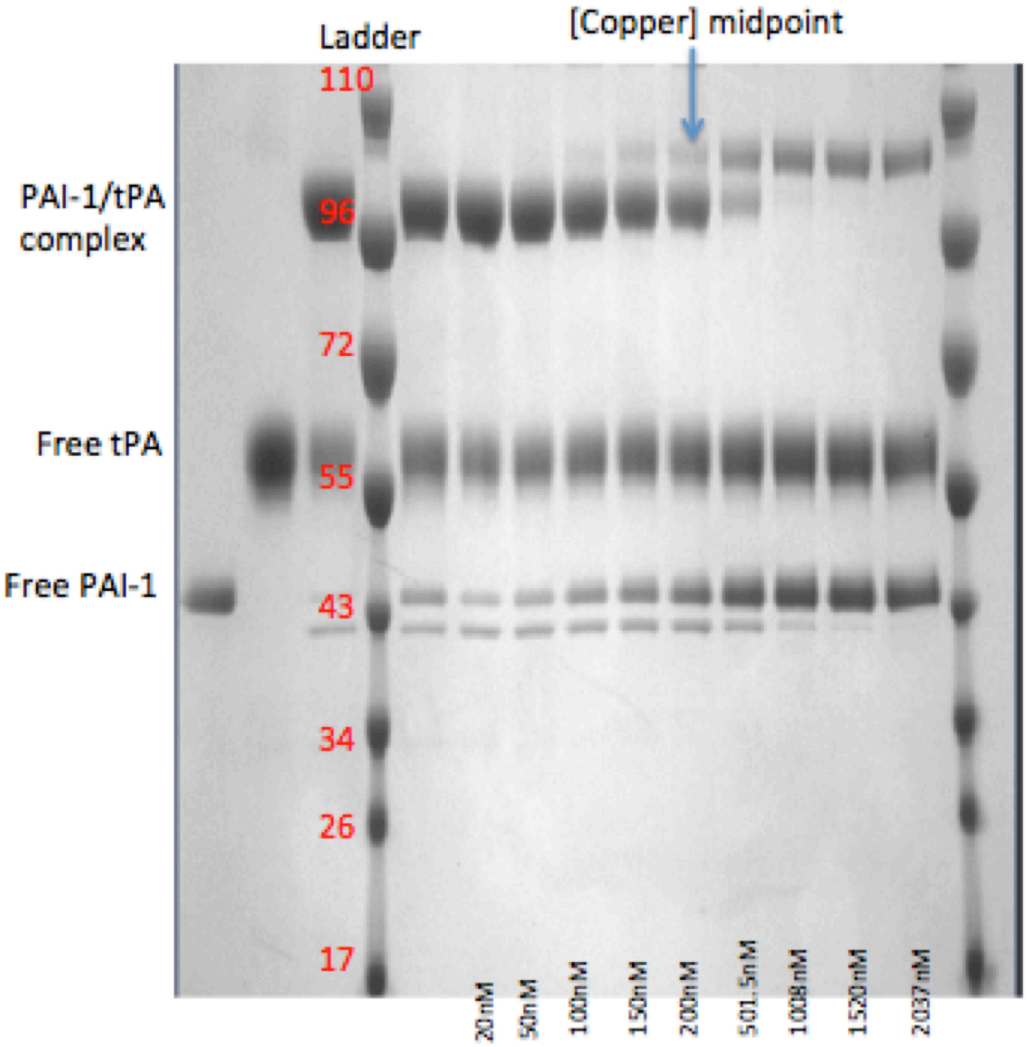

Figure 5. Example gel assay on wild type PAI-1. Free PAI-1 is in lane one. Free tPA is in lane 2. Complex formation of PAI-1 and tPA is in lane 3. The ladder is in lane 4. Lane 5 is also complex between PAI-1 and tPA. Lane 6 is PAI-1+tPA+20nM free copper. Lane 7 is PAI-1+tPA+50nM free copper. Lane 8 is PAI-1+tPA+100nM free copper. Lane 9 is PAI-1+tPA+150nM free copper. Lane 10 is PAI-1+tPA+200nM free copper. Lane 11 is PAI-1+tPA+501.5nM free copper. Lane 12 is PAI-1+tPA+1008nM free copper. Lane 13 is PAI-1+tPA+1520nM free copper. Lane 14 is PAI-1+tPA+2037nM free copper. PAI-1 and copper were incubated for 30 minutes at 37°C, followed by formation of complex by adding tPA. Samples were prepared for SDS-PAGE gel for separation and were stained by commassie blue.

interesting trends that we observed in the gel assay. First, as we increased the concentration of copper we see increasing amounts of latent PAI-1, either in the cleaved form or the latent form. This makes sense because we know that copper increases PAI-1 latency conversion. The second trend that we see is that at low concentrations of copper we observe a low amount of free tPA, and this increases with increasing copper concentrations. This is because more tPA is bound to PAI-1 in complex. The third trend we observe is at low concentrations of copper, we see high complex formation between PAI-1 and tPA. The complex formation decreases with higher concentrations of copper. All together, we can conclude that copper induces formation of latent PAI-1, accounting for less complex formation to occur as we increase copper concentrations.

From these qualitative assessments, it was apparent that complex formation decreases as the concentration of copper increases; however, we desired more analyses that would allow for comparison of wild type PAI-1 in the presence of copper to mutants we suspect to be copper binding deficient. In order to achieve the quantitative analysis, we used Image Lab to quantify band intensities at each copper concentration (Figure 6). Following this, we take the quantified band intensities of two replicates and evaluated the data using Graphpad Prism to compare variations in band intensities as a function of increasing copper concentration. The critical concentration of copper for wild type PAI-1 is 200nM free copper, as this appears to be the midpoint for the decrease of complex formation (Figure 7).

We performed a control with only tPA to determine if copper affects tPA function, in a way that would alter the interpretation of our results (Figure 8). The assays were conducted in the same fashion as the rest of the assays, except with no PAI-1. The migration of tPA is to

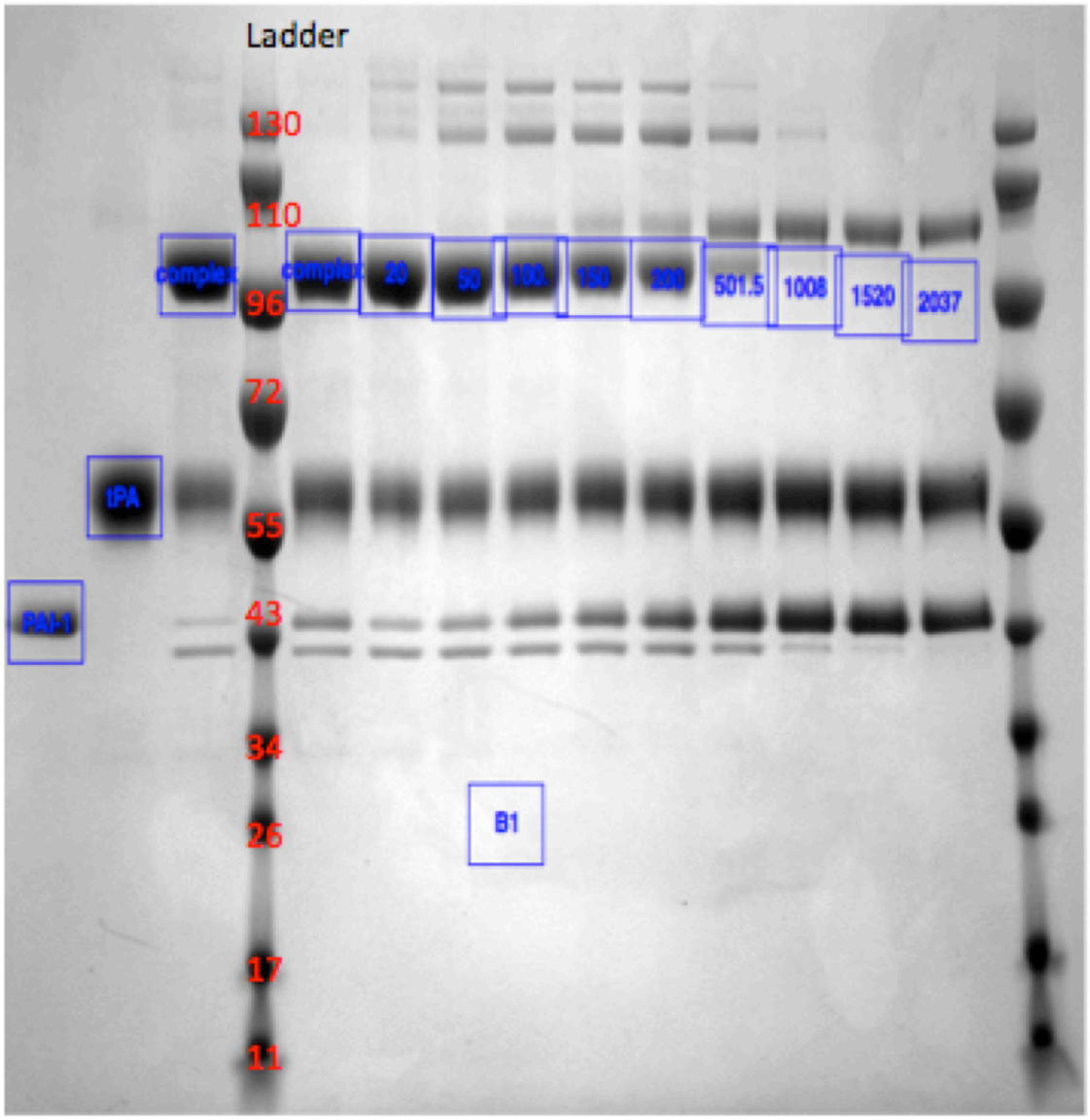

Figure 6. An example of the gel densitometry on wild type PAI-1. Each band intensity was quantified using Image Lab version 3.0. Identical boxes were drawn around PAI-1, tPA, and their complex formation at each metal concentration as shown by the blue boxes. B1 was the background subtraction for all other experimental conditions. We generated a report with the band intensities, averaged the duplicates and put them into Graphpad Prism.

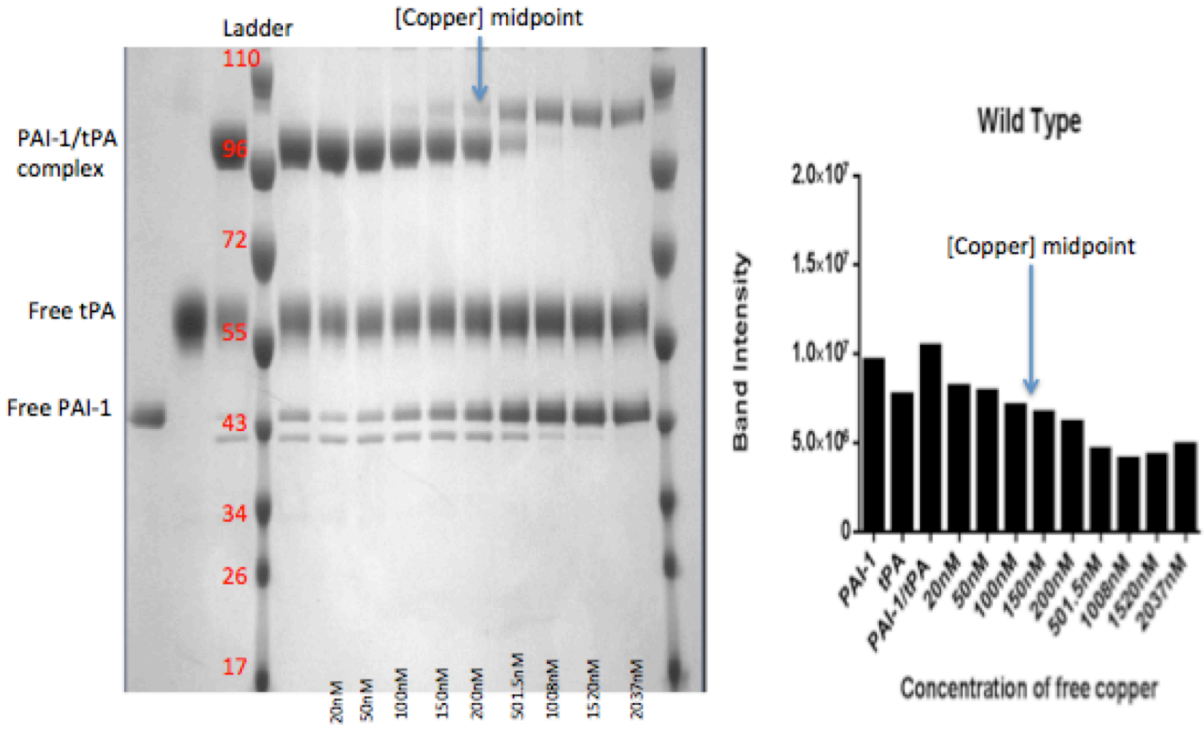

Figure 7. Example gel assay on wild type PAI-1. Free PAI-1 is in lane one. Free tPA is in lane 2. Complex formation of PAI-1 and tPA is in lane 3. The ladder is in lane 4. Lane 5 is also complex between PAI-1 and tPA. Lane 6 is PAI-1+tPA+20nM free copper. Lane 7 is PAI-1+tPA+50nM free copper. Lane 8 is PAI-1+tPA+100nM free copper. Lane 9 is PAI-1+tPA+150nM free copper. Lane 10 is PAI-1+tPA+200nM free copper. Lane 11 is PAI-1+tPA+501.5nM free copper. Lane 12 is PAI-1+tPA+1008nM free copper. Lane 13 is PAI-1+tPA+1520nM free copper. Lane 14 is PAI-1+tPA+2037nM free copper. PAI-1 and copper were incubated for 30 minutes at 37°C, followed by formation of complex by adding tPA. Samples were prepared for SDS-PAGE gel for separation and were stained by commassie blue. The band intensities were averaged and plotted in bar graphs in Graphpad Prism for quantification.

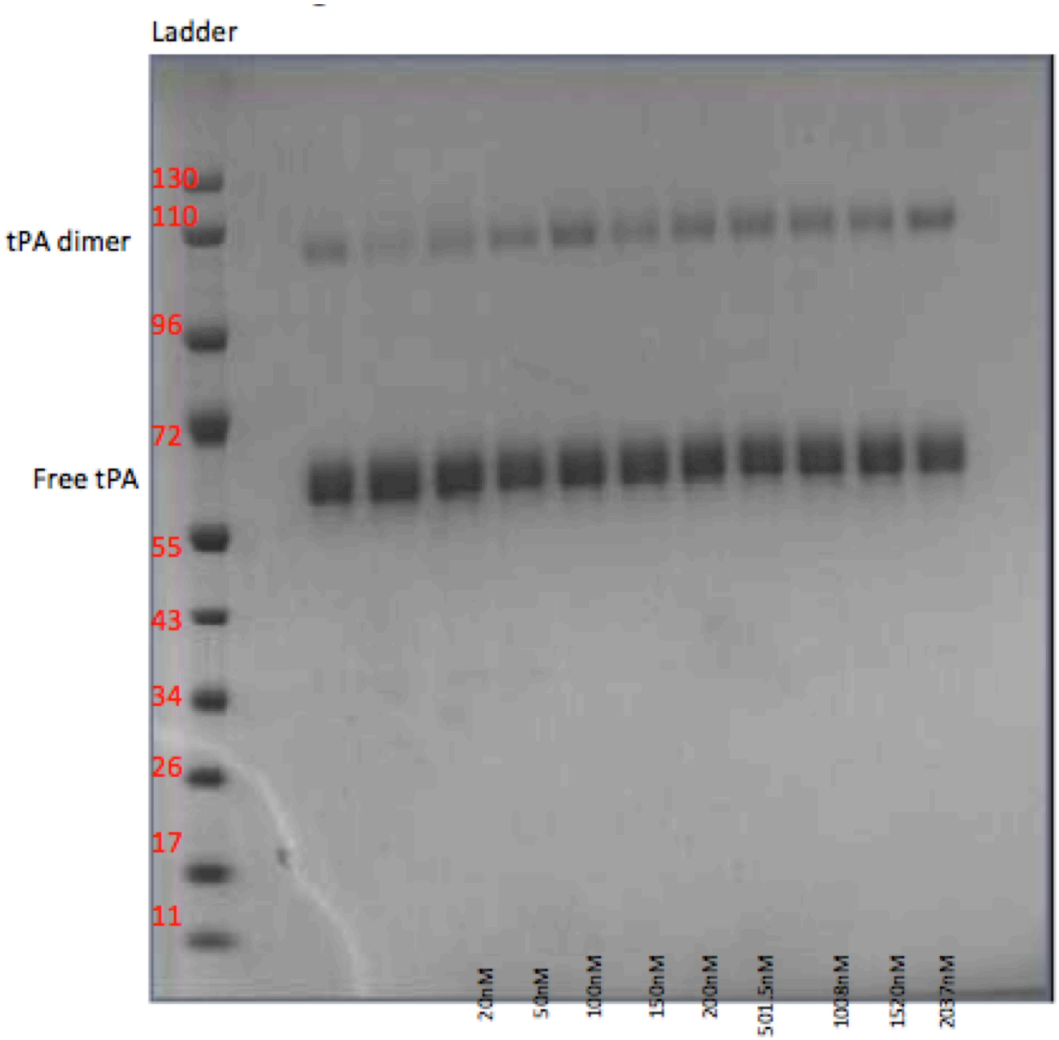

Figure 8. Control assay to determine if copper has an effect on tPA. The ladder is in lane 1. Lane 2 is only buffer. Lane 3 and 4 are tPA only. Lane 5 is tPA+20nM free copper. Lane 6 is tPA+50nM free copper. Lane 7 is tPA+100nM free copper. Lane 8 is tPA+150nM free copper. Lane 9 is tPA+200nM free copper. Lane 10 is tPA+501.5nM free copper. Lane 11 is tPA+1008nM free copper. Lane 12 is tPA+1520nM free copper. Lane 13 is tPA+2037nM free copper.

slightly lower than the 72kDa standard in the ladder, consistent with the size of the protein which is 70kDa. We observed a small band around the 110kDa protein standard in the ladder, consistent with a dimer formation of tPA (Both of the bands do not run exactly to size; they ru slightly smaller than the theoretical size). The addition of copper in the concentration range used in the experiments had no effect on the migration or intensity of either tPA band. Thus, we conclude that metal effects that we observe in this assay are predominantly from effects on PAI-1.

We then compared wild type PAI-1 to the N-terminal histidine mutants (H2A and H3A) to determine if these residues may be involved in copper coordination to accelerate latency transition. If they were involved, we expect to see complex formation at higher copper concentrations compared to wild type PAI-1 due weakened binding. To our surprise, the midpoint for the decrease for complex formation was 100nM free copper for both H2A and H3A (Figures 9 and 10). This suggests that the N-terminal histidines are not involved in copper binding that leads to accelerated latency conversion and altered complex formation. We also have a double mutant in which both histidines are converted to alanines (H2A/H3A). It is possible that both histidines must be absent for copper binding to be significantly altered. The single point mutations actually caused more sensitivity to copper than wild type PAI-1. To further investigate this finding, it will be important to run a control experiment to compare the stability of wild type PAI-1 and the mutants PAI-1 in the absence of copper to determine what affect the individual mutations have on intrinsic protein stability. The mutations are located in a hydrophobic pocket and alterations to the region may change the structure and overall stability of PAI-1.

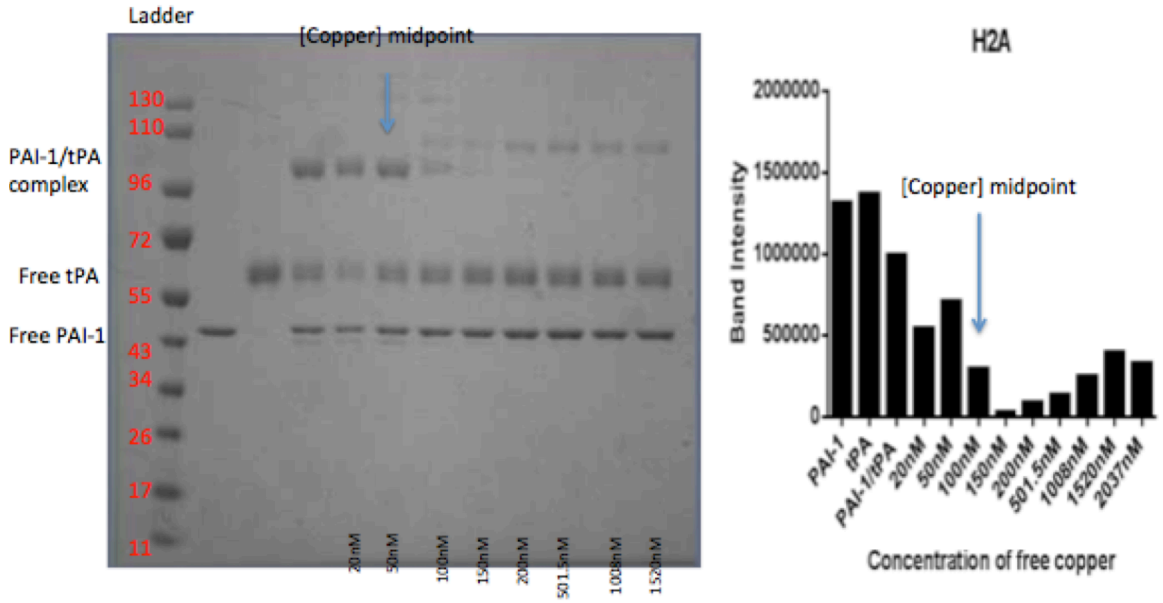

Figure 9. Gel assay on H2A PAI-1. The ladder is in lane 1. Free PAI-1 is in lane 2. Free tPA is in lane 3. Complex formation of PAI-1 and tPA is in lane 4. Lane 5 is PAI-1+tPA+20nM free copper. Lane 6 is PAI-1+tPA+50nM free copper. Lane 7 is PAI-1+tPA+100nM free copper. Lane 8 is PAI-1+tPA+150nM free copper. Lane 9 is PAI-1+tPA+200nM free copper. Lane 10 is PAI-1+tPA+501.5nM free copper. Lane 11 is PAI-1+tPA+1008nM free copper. Lane 12 is PAI-1+tPA+1520nM free copper. Lane 13 is PAI-1+tPA+2037nM free copper. PAI-1 and copper were incubated for 30 minutes at 37°C, followed by formation of complex by adding tPA. Samples were prepared for SDS-PAGE gel for separation and were stained by commassie blue. The band intensities were averaged and plotted in bar graphs in Graphpad Prism for quantification.

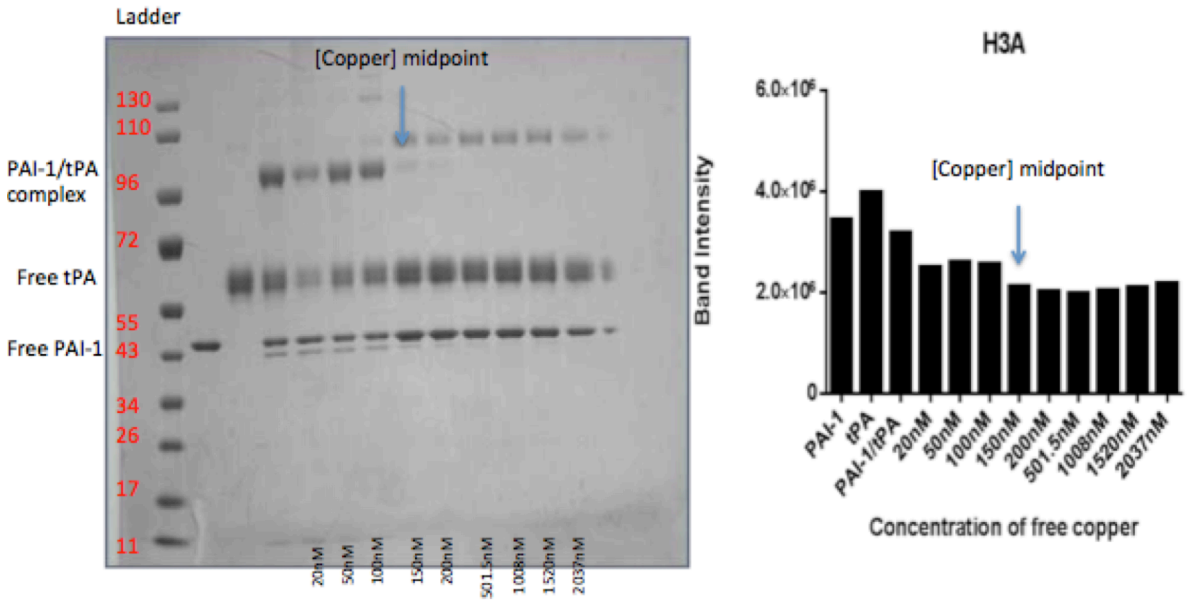

Figure 10. Gel assay on H3A PAI-1. The ladder is in lane 1. Free PAI-1 is in lane 2. Free tPA is in lane 3. Complex formation of PAI-1 and tPA is in lane 4. Lane 5 is PAI-1+tPA+20nM free copper. Lane 6 is PAI-1+tPA+50nM free copper. Lane 7 is PAI-1+tPA+100nM free copper. Lane 8 is PAI-1+tPA+150nM free copper. Lane 9 is PAI-1+tPA+200nM free copper. Lane 10 is PAI-1+tPA+501.5nM free copper. Lane 11 is PAI-1+tPA+1008nM free copper. Lane 12 is PAI-1+tPA+1520nM free copper. Lane 13 is PAI-1+tPA+2037nM free copper. PAI-1 and copper were incubated for 30 minutes at 37°C, followed by formation of complex by adding tPA. Samples were prepared for SDS-PAGE gel for separation and were stained by commassie blue. The band intensities were averaged and plotted in bar graphs in Graphpad Prism for quantification

Finally, we compared wild type PAI-1 to several single mutants (E350T, E212A, E242A), as well as a double (D222A/E350A) and triple mutant (D222A/E350A/E212A) all located in the gate region of PAI-1. The gate region is already known to be flexible and important in the latency transition process (Egelund, Schousboe et al. 1997). We hypothesized that copper may bind and stabilize this region using the aforementioned residues. Some of the gate region residues conferred a modest change in the critical concentration of copper compared to wild type PAI-1. These observations provide the foundation for interesting studies in the future. The mutant E350T PAI-1 has a midpoint for the decrease in complex formation at 200nM free copper, which is comparable to wild type PAI-1 (Figure 11). However, the mutant E212A has a midpoint for the decrease in complex formation at ~500nM free copper, a slightly higher concentration than that observed with wild type PAI-1 (Figure 12). Similarly, we observe a midpoint for the decrease in complex formation of ~500nM free copper in E242A PAI-1 (Figure 13). These are modest alterations, but they indicate that these residues may play a role in copper coordination that accelerates latency conversion.

Usually, copper binds in tetrahedral geometry, using four groups to coordinate the metal. For experiments on single mutations, we can expect only a modest effect on copper binding. However, we reasoned that a combination of double or triple mutations would likely produce more substantial effects. To test this notion, we studied PAI-1 with combinations of D222A/E350A (Figure 14) or D222A/E350A/E212A mutations (Figure 15). The midpoint for the decrease in complex formation for D222A/E350A is 200nM free copper. This was not surprising because we had observed that E350T did not alter copper binding, but we had yet to test D222A. However, the triple mutant also had a midpoint for the decrease in complex formation

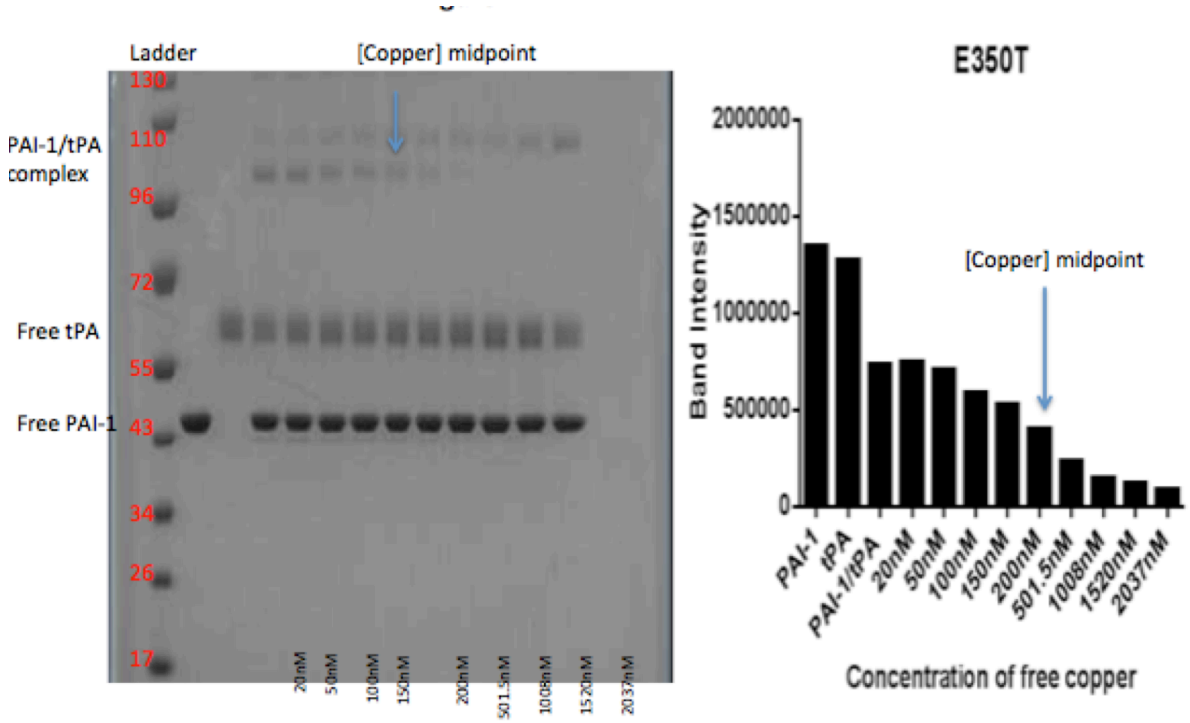

Figure 11. Gel assay on E350T PAI-1. The ladder is in lane 1. Free PAI-1 is in lane 2. Free tPA is in lane 3. Complex formation of PAI-1 and tPA is in lane 4. Lane 5 is PAI-1+tPA+20nM free copper. Lane 6 is PAI-1+tPA+50nM free copper. Lane 7 is PAI-1+tPA+100nM free copper. Lane 8 is PAI-1+tPA+150nM free copper. Lane 9 is PAI-1+tPA+200nM free copper. Lane 10 is PAI-1+tPA+501.5nM free copper. Lane 11 is PAI-1+tPA+1008nM free copper. Lane 12 is PAI-1+tPA+1520nM free copper. Lane 13 is PAI-1+tPA+2037nM free copper. PAI-1 and copper were incubated for 30 minutes at 37°C, followed by formation of complex by adding tPA. Samples were prepared for SDS-PAGE gel for separation and were stained by commassie blue. The band intensities were averaged and plotted in bar graphs in Graphpad Prism for quantification

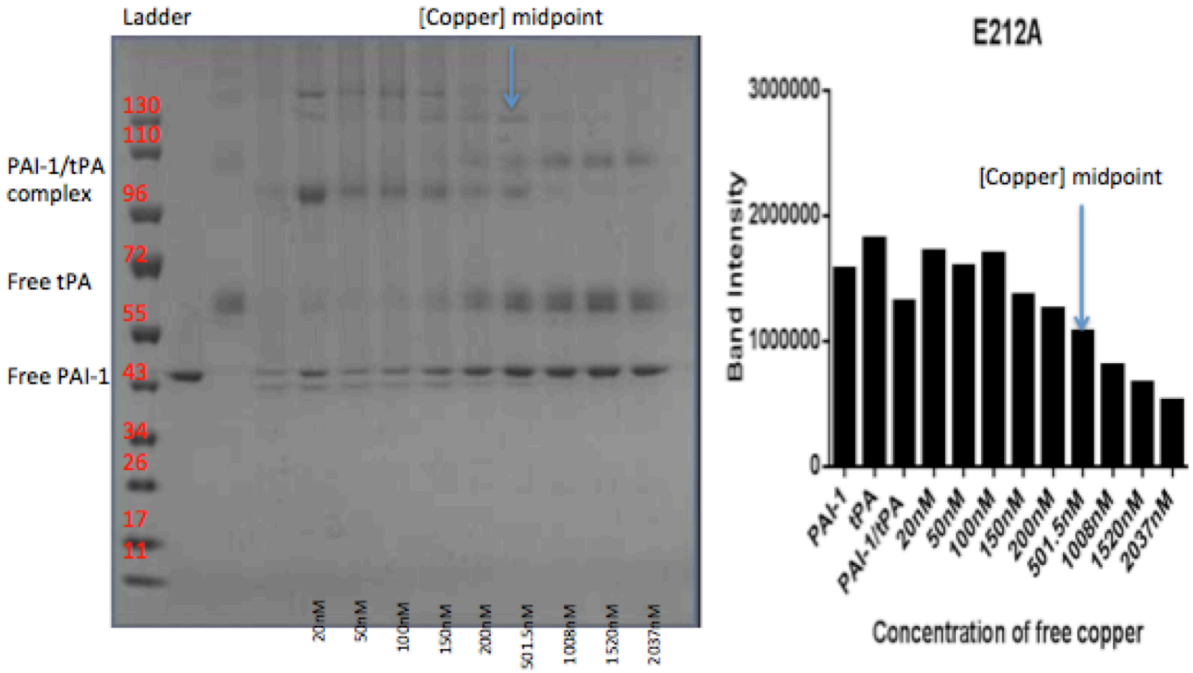

Figure 12. Gel assay on E212A PAI-1. The ladder is in lane 1. Free PAI-1 is in lane 2. Free tPA is in lane 3. Complex formation of PAI-1 and tPA is in lane 4. Lane 5 is PAI-1+tPA+20nM free copper. Lane 6 is PAI-1+tPA+50nM free copper. Lane 7 is PAI-1+tPA+100nM free copper. Lane 8 is PAI-1+tPA+150nM free copper. Lane 9 is PAI-1+tPA+200nM free copper. Lane 10 is PAI-1+tPA+501.5nM free copper. Lane 11 is PAI-1+tPA+1008nM free copper. Lane 12 is PAI-1+tPA+1520nM free copper. Lane 13 is PAI-1+tPA+2037nM free copper. PAI-1 and copper were incubated for 30 minutes at 37°C, followed by formation of complex by adding tPA. Samples were prepared for SDS-PAGE gel for separation and were stained by commassie blue. The band intensities were averaged and plotted in bar graphs in Graphpad Prism for quantification

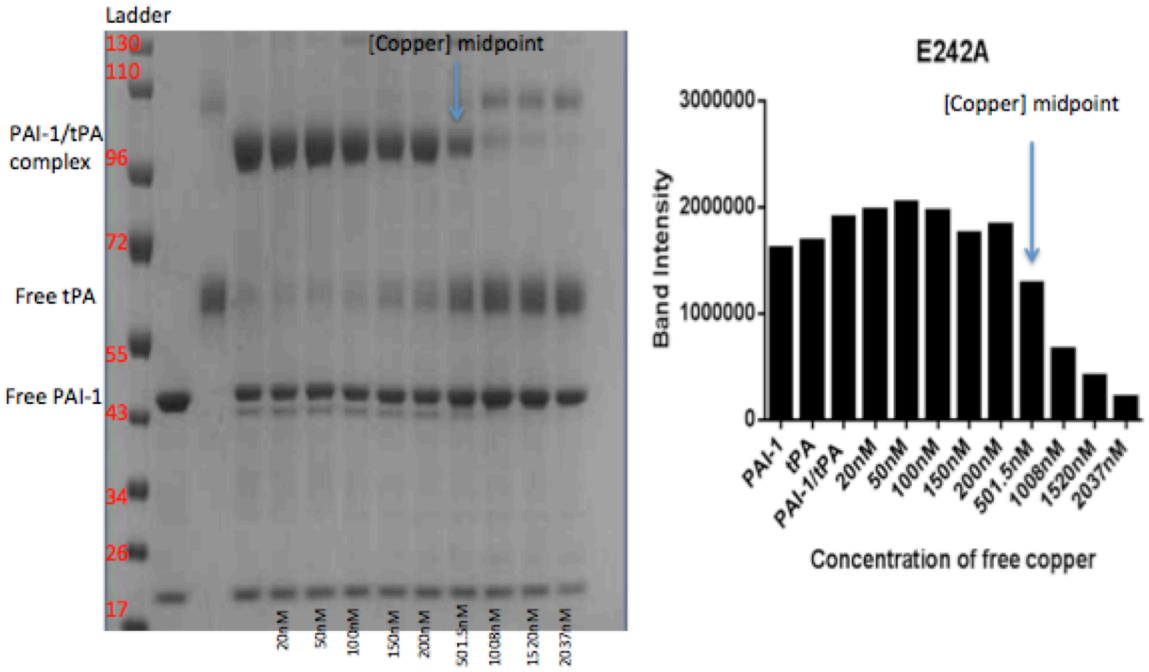

Figure 13. Gel assay on E242A PAI-1. The ladder is in lane 1. Free PAI-1 is in lane 2. Free tPA is in lane 3. Complex formation of PAI-1 and tPA is in lane 4. Lane 5 is PAI-1+tPA+20nM free copper. Lane 6 is PAI-1+tPA+50nM free copper. Lane 7 is PAI-1+tPA+100nM free copper. Lane 8 is PAI-1+tPA+150nM free copper. Lane 9 is PAI-1+tPA+200nM free copper. Lane 10 is PAI-1+tPA+501.5nM free copper. Lane 11 is PAI-1+tPA+1008nM free copper. Lane 12 is PAI-1+tPA+1520nM free copper. Lane 13 is PAI-1+tPA+2037nM free copper. PAI-1 and copper were incubated for 30 minutes at 37°C, followed by formation of complex by adding tPA. Samples were prepared for SDS-PAGE gel for separation and were stained by commassie blue. The band intensities were averaged and plotted in bar graphs in Graphpad Prism for quantification.

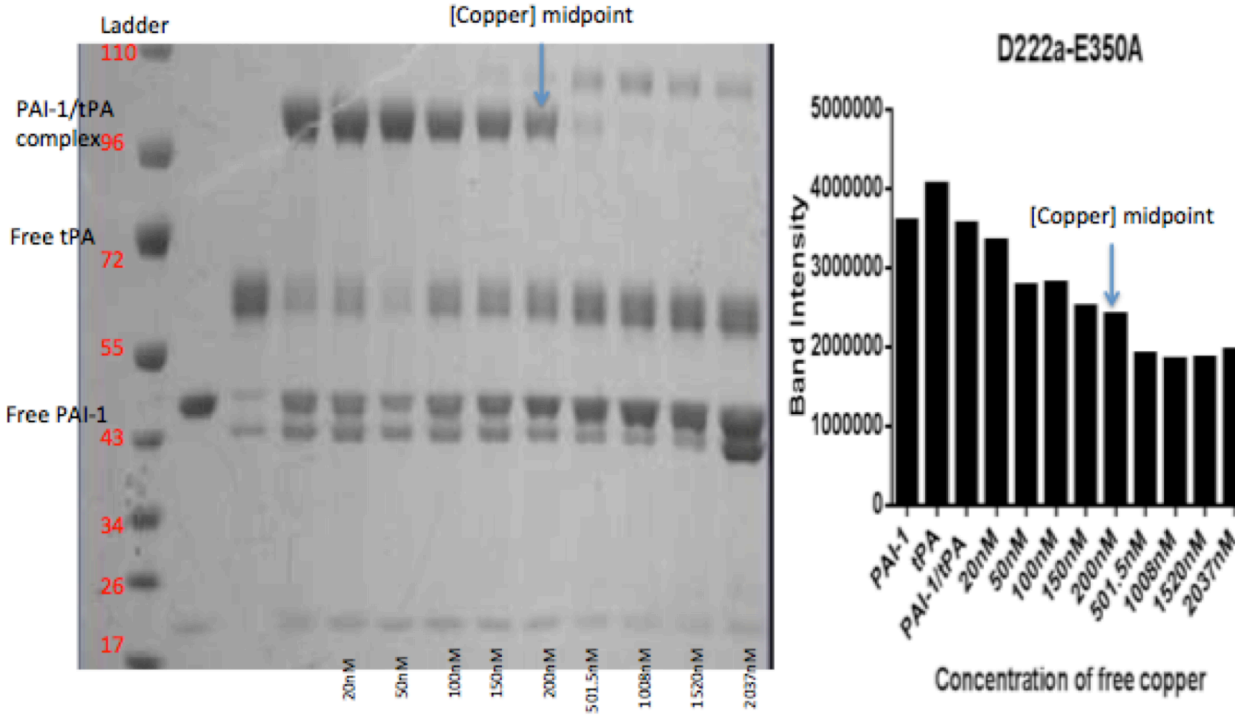

Figure 14. Gel assay on D222A/E350A PAI-1. The ladder is in lane 1. Free PAI-1 is in lane 2. Free tPA is in lane 3. Complex formation of PAI-1 and tPA is in lane 4. Lane 5 is PAI-1+tPA+20nM free copper. Lane 6 is PAI-1+tPA+50nM free copper. Lane 7 is PAI-1+tPA+100nM free copper. Lane 8 is PAI-1+tPA+150nM free copper. Lane 9 is PAI-1+tPA+200nM free copper. Lane 10 is PAI-1+tPA+501.5nM free copper. Lane 11 is PAI-1+tPA+1008nM free copper. Lane 12 is PAI-1+tPA+1520nM free copper. Lane 13 is PAI-1+tPA+2037nM free copper. PAI-1 and copper were incubated for 30 minutes at 37°C, followed by formation of complex by adding tPA. Samples were prepared for SDS-PAGE gel for separation and were stained by commassie blue. The band intensities were averaged and plotted in bar graphs in Graphpad Prism for quantification.

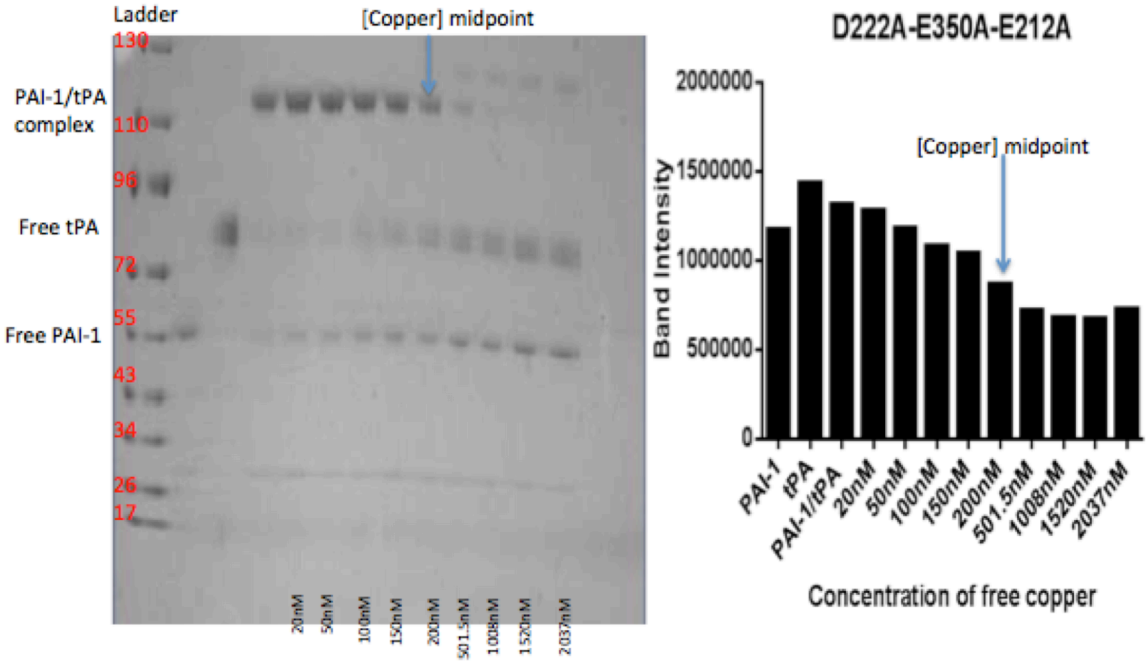

Figure 15. Gel assay on D222A/E350A/E212A PAI-1. The ladder is in lane 1. Free PAI-1 is in lane 2. Free tPA is in lane 3. Complex formation of PAI-1 and tPA is in lane 4. Lane 5 is PAI-1+tPA+20nM free copper. Lane 6 is PAI-1+tPA+50nM free copper. Lane 7 is PAI-1+tPA+100nM free copper. Lane 8 is PAI-1+tPA+150nM free copper. Lane 9 is PAI-1+tPA+200nM free copper. Lane 10 is PAI-1+tPA+501.5nM free copper. Lane 11 is PAI-1+tPA+1008nM free copper. Lane 12 is PAI-1+tPA+1520nM free copper. Lane 13 is PAI-1+tPA+2037nM free copper. PAI-1 and copper were incubated for 30 minutes at 37°C, followed by formation of complex by adding tPA. Samples were prepared for SDS-PAGE gel for separation and were stained by commassie blue. The band intensities were averaged and plotted in bar graphs in Graphpad Prism for quantification

of 200nM free copper. This result was unexpected because we previously observed changes due to the incorporation of E212A PAI-1.

In conclusion, we have developed an assay to directly monitor the complex formation of PAI-1 and tPA in the presence of a range of copper concentrations. We observed a decrease in PAI-1/tPA complex formation as the concentration of copper increases. After measuring band intensities, we could determine the critical concentration in which copper accelerates PAI-1 conversion the latent form, thereby unable to form complex with tPA. We compared wild type PAI-1 to mutants that we propose to participate in binding metals. We observed expected differences in some of the gate regions mutants (E212A and E242A). We plan to continue to investigate binding affinity on PAI-1 with these mutations using other more traditional techniques, i.e. isothermal titration calorimetry, to determine if affinity differences exist. We also observed no effect due to mutations of the N-terminal histidines (H2A and H3A), indicating that these residues are not involved in binding metals that affect PAI-1 stability.

In the future, other individuals in the laboratory will complete all the possible mutations combinations, including D22A, H2A/H3A and also E212A/E242A, and will be able to employ this gel-based technique to compare with wild type PAI-1. Any mutations that reveal a difference will then be tested using isothermal titration calorimetry to further characterize differences in metal-binding affinity. It also may be necessary to expand our search for metal binding sites on PAI-1 using computational techniques and other experimental methods if these studies on targeted mutations prove unsuccessful.

Works cited

Berg JM, Tymoczko JL, Stryer L. Biochemistry. 6th edition. New York: W H Freeman; 2007.

Bleackley, M. R. and R. T. Macgillivray (2011). "Transition metal homeostasis: from yeast to human disease." Biometals **24**(5): 785-809.

Blouse, G. E., D. M. Dupont, C. R. Schar, J. K. Jensen, K. H. Minor, J. Y. Anagli, H. Gardsvoll, M. Ploug, C. B. Peterson and P. A. Andreasen (2009). "Interactions of plasminogen activator inhibitor-1 with vitronectin involve an extensive binding surface and induce mutual conformational rearrangements." Biochemistry **48**(8): 1723-1735.

Buck, M. J. and W. R. Atchley (2005). "Networks of coevolving sites in structural and functional domains of serpin proteins." Mol Biol Evol **22**(7): 1627-1634.

Dellas, C. and D. J. Loskutoff (2005). "Historical analysis of PAI-1 from its discovery to its potential role in cell motility and disease." Thromb Haemost **93**(4): 631-640.

Dudev, T. and C. Lim (2008). "Metal binding affinity and selectivity in metalloproteins: insights from computational studies." Annu Rev Biophys **37**: 97-116.

Dupont, D. M., G. E. Blouse, M. Hansen, L. Mathiasen, S. Kjelgaard, J. K. Jensen, A. Christensen, A. Gils, P. J. Declerck, P. A. Andreasen and T. Wind (2006). "Evidence for a pre-latent form of the serpin plasminogen activator inhibitor-1 with a detached beta-strand 1C." J Biol Chem **281**(47): 36071-36081.

Egelund, R., S. L. Schousboe, L. Sottrup-Jensen, K. W. Rodenburg and P. A. Andreasen (1997). "Type-1 plasminogen-activator inhibitor -- conformational differences between latent, active, reactive-centre-cleaved and plasminogen-activator-complexed forms, as probed by proteolytic susceptibility." Eur J Biochem **248**(3): 775-785.

Gettins, P. G. (2002). "The F-helix of serpins plays an essential, active role in the proteinase inhibition mechanism." FEBS Lett **523**(1-3): 2-6.
Horn, N. A., G. B. Hurst, A. Mayasundari, N. A. Whittemore, E. H. Serpersu and C. B. Peterson (2004). "Assignment of the four disulfides in the N-terminal somatomedin B domain of native vitronectin isolated from human plasma." J Biol Chem **279**(34): 35867-35878.

Iwaki, T., T. Urano and K. Umemura (2012). "PAI-1, progress in understanding the clinical problem and its aetiology." Br J Haematol **157**(3): 291-298.

Jensen, J. K., L. C. Thompson, J. C. Bucci, P. Nissen, P. G. Gettins, C. B. Peterson, P. A. Andreasen and J. P. Morth (2011). "Crystal structure of plasminogen activator inhibitor-1 in an active conformation with normal thermodynamic stability." J Biol Chem **286**(34): 29709-29717.

Jensen, J. K., T. Wind and P. A. Andreasen (2002). "The vitronectin binding area of plasminogen activator inhibitor-1, mapped by mutagenesis and protection against an inactivating organochemical ligand." FEBS Lett **521**(1-3): 91-94.

Kodama, H., C. Fujisawa and W. Bhadhprasit (2012). "Inherited copper transport disorders: biochemical mechanisms, diagnosis, and treatment." Curr Drug Metab **13**(3): 237-250.

Kramer, M. L., H. D. Kratzin, B. Schmidt, A. Romer, O. Windl, S. Liemann, S. Hornemann and H. Kretzschmar (2001). "Prion protein binds copper within the physiological concentration range." J Biol Chem **276**(20): 16711-16719.

Lynn, G. W., W. T. Heller, A. Mayasundari, K. H. Minor and C. B. Peterson (2005). "A model for the three-dimensional structure of human plasma vitronectin from small-angle scattering measurements." Biochemistry **44**(2): 565-574.

Minor, K. H. and C. B. Peterson (2002). "Plasminogen activator inhibitor type 1 promotes the self-association of vitronectin into complexes exhibiting altered incorporation into the extracellular matrix." J Biol Chem **277**(12): 10337-10345.

Miotto, M. C., E. E. Rodriguez, A. A. Valiente-Gabioud, V. Torres-Monserrat, A. Binolfi, L. Quintanar, M. Zweckstetter, C. Griesinger and C. O. Fernandez (2014). "Site-Specific Copper-Catalyzed Oxidation of alpha-Synuclein: Tightening the Link between Metal Binding and Protein Oxidative Damage in Parkinson's Disease." Inorg Chem.

Olson, S. T. and P. G. Gettins (2011). "Regulation of proteases by protein inhibitors of the serpin superfamily." Prog Mol Biol Transl Sci **99**: 185-240.

Olson, S. T., R. Swanson, D. Day, I. Verhamme, J. Kvassman and J. D. Shore (2001). "Resolution of Michaelis complex, acylation, and conformational change steps in the reactions of the serpin, plasminogen activator inhibitor-1, with tissue plasminogen activator and trypsin." Biochemistry **40**(39): 11742-11756.

Palm-Espling, M. E., M. S. Niemiec and P. Wittung-Stafshede (2012). "Role of metal in folding and stability of copper proteins in vitro." Biochim Biophys Acta **1823**(9): 1594-1603.

Stoop, A. A., F. Lupu and H. Pannekoek (2000). "Colocalization of thrombin, PAI-1, and vitronectin in the atherosclerotic vessel wall: A potential regulatory mechanism of thrombin activity by PAI-1/vitronectin complexes." Arterioscler Thromb Vasc Biol **20**(4): 1143-1149.

Stout, T. J., H. Graham, D. I. Buckley and D. J. Matthews (2000). "Structures of active and latent PAI-1: a possible stabilizing role for chloride ions." Biochemistry **39**(29): 8460-8469.

Sui, G. C., H. Mangs and B. Wiman (1999). "The role of His(143) for the pH-dependent stability of plasminogen activator inhibitor-1." Biochim Biophys Acta **1434**(1): 58-63.

Szent-Gyorgyi, A. G. (1975). "Calcium regulation of muscle contraction." Biophys J **15**(7): 707-723.
Thompson, L. C., S. Goswami, D. S. Ginsberg, D. E. Day, I. M. Verhamme and C. B. Peterson (2010). "Metals affect the structure and activity of human plasminogen activator inhibitor-1." Protein Sci.

Thompson, L. C., S. Goswami and C. B. Peterson (2010). "Metals affect the structure and activity of human plasminogen activator inhibitor-1." Protein Sci.

Van De Craen, B., P. J. Declerck and A. Gils (2012). "The Biochemistry, Physiology and Pathological roles of PAI-1 and the requirements for PAI-1 inhibition in vivo." Thromb Res **130**(4): 576-585.

Zhou, A., J. A. Huntington, N. S. Pannu, R. W. Carrell and R. J. Read (2003). "How vitronectin binds PAI-1 to modulate fibrinolysis and cell migration." Nat Struct Biol **10**(7): 541-544.